Materials Today Bio 31 (2025) 101504

Contents lists available at ScienceDirect

Materials Today Bio

journal homepage: www.journals.elsevier.com/materials-today-bio

Recent advances in iontophoresis-assisted microneedle devices for transdermal biosensing and drug delivery

Gaobo Wang [a,b], Natsuho Moriyama [c], Soichiro Tottori [b], Matsuhiko Nishizawa [b,c,*]

[a] Department of Biomedical Engineering, School of Medical Engineering, Xinxiang Medical University, Xinxiang, 453003, China
[b] Department of Finemechanics, Graduate School of Engineering, Tohoku University, 6-6-1 Aramaki Aoba, Aoba-ku, Sendai, 980-8579, Japan
[c] Department of Biomedical Engineering, Graduate School of Biomedical Engineering, Tohoku University, 6-6-4 Aramaki Aoba, Aoba-ku, Sendai, 980-8579, Japan

ARTICLE INFO

Keywords:
Iontophoresis
Microneedle
Transdermal sensing
Drug delivery
Closed-loop system

ABSTRACT

Integrating advanced manufacturing techniques and nanotechnology with cutting-edge materials has driven significant progress in global healthcare. Microneedles, recognized for their minimally invasive approach to transdermal sensing and drug delivery, achieve enhanced functionality when combined with iontophoresis. Iontophoresis-assisted microneedles have emerged as an innovative solution, enabling real-time biosensing and precise drug delivery within closed-loop systems. These integrated platforms represent a major advancement in personalized medicine, allowing dynamic therapeutic adjustments based on continuous feedback. This review highlights the latest developments in iontophoresis-assisted microneedles for transdermal biosensing, drug delivery, and closed-loop applications. It delves into the mechanisms of iontophoresis, assesses its advantages and limitations, and explores future directions for these transformative technologies.

1. Introduction

Iontophoresis (IP), a method utilizing mild electrical currents to drive ions or flow, stands as a testament to the fusion of science and medical innovation [1–4]. The foundational principles of IP were established in the 19th century through early studies of galvanic effects and electrophoresis [5]. At its core, IP operates on the principle of electromigration (or electrophoresis, EP), electroosmosis and the increased permeability of membranes or skin due to the flow of electric current, leveraging the charged ions' movement in an electric field to drive the transport of agents across biological membranes or skin [6]. Electroosmosis generates interstitial fluid (ISF) flow from anode to cathode due to the preferential movement of cations in the negatively charged skin tissue. The late 1990s saw the advent of biosensors that incorporated reverse iontophoresis (RI) to facilitate the detection of various analytes [7–9]. Researchers developed devices that could measure glucose levels in ISF by driving glucose oxidase and other sensing elements. On the other hand, the versatility of IP has led to its widespread adoption for drug delivery. In dermatology, it is used for transdermal delivery of medications, ranging from local anesthetics to anti-inflammatory agents, offering a non-invasive alternative to traditional injection methods [10,11]. Similarly, in physical therapy, IP is employed for the localized treatment of musculoskeletal disorders, such as tendonitis and bursitis, providing targeted relief to patients [12].

Microneedles (MNs) have emerged as a groundbreaking approach in biosensing and drug delivery [13–16]. These MNs can be fabricated from various materials, including silicon, metal, and polymers, each offering unique properties such as flexibility, biocompatibility, and dissolvability [17,18]. Depending on the materials and structures, MNs can be categorized into solid, hollow, hydrogel, dissolving and porous MNs [19–21]. By incorporating biosensors directly into MNs, the devices capable of detecting a wide range of analytes, including glucose, lactate, and biomarkers indicative of various diseases have been developed [22–24]. These advancements hold promises for continuous monitoring of health parameters, early disease detection, and personalized medicine. Moreover, MNs have demonstrated remarkable versatility in the drug delivery field, enabling precise control over drug dosage and release kinetics while minimizing patient discomfort and side effects [25]. The integration of MNs with IP represents a transformative approach, addressing key challenges in non-invasive biomarker monitoring and on-demand drug delivery. This synergy also enables the development of smart, closed-loop systems that provide personalized, real-time therapies, offering significant advances in managing chronic conditions such as diabetes. Despite its promise, critical challenges

* Corresponding author. Department of Finemechanics, Graduate School of Engineering, Tohoku University, 6-6-1 Aramaki Aoba, Aoba-ku, Sendai, 980-8579, Japan.
E-mail address: nishizawa@tohoku.ac.jp (M. Nishizawa).

https://doi.org/10.1016/j.mtbio.2025.101504
Received 18 November 2024; Received in revised form 5 January 2025; Accepted 18 January 2025
Available online 19 January 2025

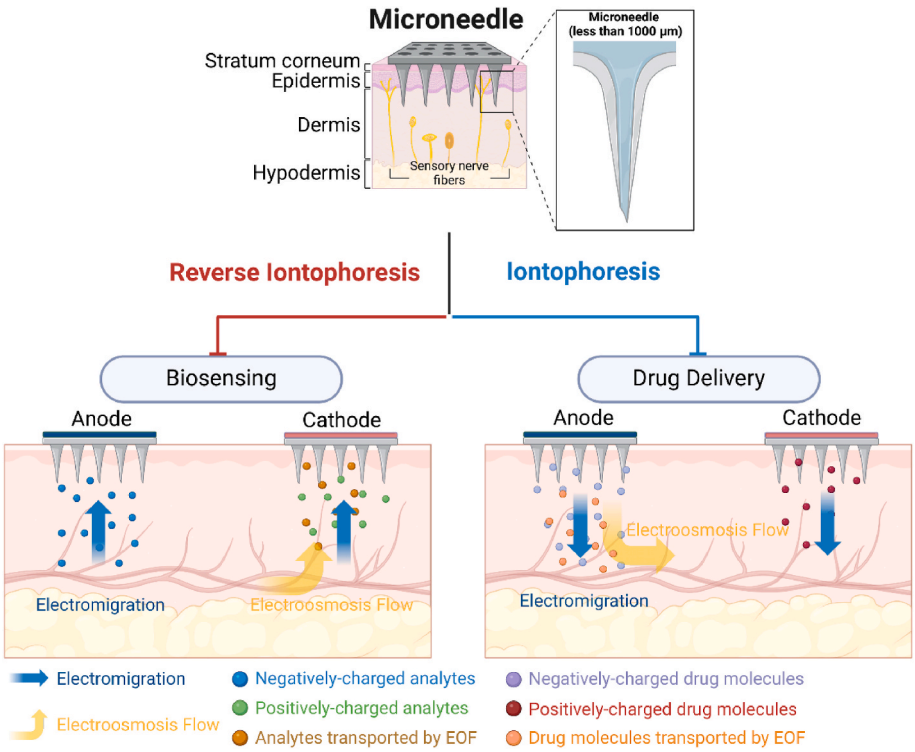

Fig. 1. Schematic illustration of mechanisms of IP and RI for transdermal biosensing and drug delivery applications.

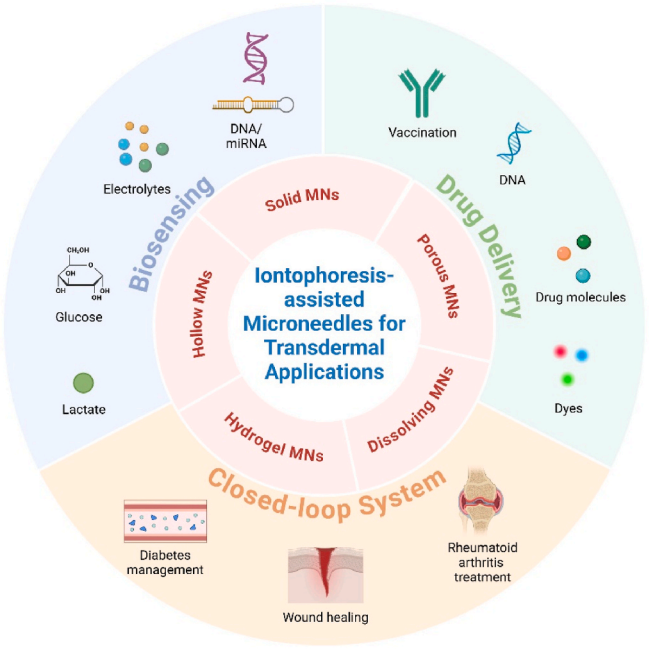

Fig. 2. An overview of IP-assisted MNs devices for diverse transdermal applications including biosensing, drug delivery and closed-loop systems.

remain, including variations in skin properties, electrochemical interference, device complexity, and power supply limitations, which must be overcome to unlock the full potential of this innovative technology. As MNs continue to evolve, researchers are exploring novel techniques and improving existing designs [26–28]. Fig. 1 illustrates the mechanisms of IP and RI through MNs for transdermal biosensing and drug delivery applications. To date, transdermal health monitoring and drug delivery have been reviewed in previous reports from different views [29–31]. For example, Saifullah et al. systematically sorted the MNs-based ISF sampling strategy [32]. Wang et al. summarized MNs-based glucose monitoring [33] and Zheng et al. reviewed the development of RI-assisted flexible electronics [34]. In the drug delivery field, Helmy et al. reviewed the iontophoretic drug delivery devices for different tissues and organs [26]. Zhang et al. summarized the wearable glucose monitoring and implantable drug delivery systems for diabetes management [35]. However, to the best of our knowledge, little attention has been paid to IP-assisted MNs devices and their applications for transdermal biosensing, drug delivery and closed-loop systems.

In this review, we systematically summarized the recent advancement of different types of MNs and their integration with IP or RI techniques (Fig. 2). In addition, their applications in transdermal biosensing, drug delivery and closed-loop systems for smart transdermal therapeutic applications will be discussed. In summary, IP-assisted MNs represent a versatile and powerful platform for enhanced transdermal therapy with patient-friendly interfaces. They offer potential for integration with wearable health monitoring devices, expand the range of deliverable drugs and enable precise control. As this field advances, it promises to bring more personalized and effective treatments to patients across diverse medical fields.

2. Mechanisms of iontophoresis and reverse iontophoresis

2.1. Iontophoresis

Iontophoresis is a method that uses an electrical potential difference (typically a low-intensity current of 0.5 mA/cm^2 or less) to enhance the movement of ions across biological membranes, usually the skin. Drug molecules (ionic or non-ionic) are driven into the skin via an electrochemical gradient generated by the electric field [36]. The total flux of a solute (J) across the skin is the sum of the contributions from electrophoresis (J_{EP}), electroosmosis (J_{EO}), and passive diffusion (J_p):

$$J = J_{EP} + J_{EO} + J_p \quad (1)$$

2.1.1. Electrophoresis

Electrophoresis refers to the movement of ions through the skin due to the applied electric field. The flux of electrons is converted into ionic fluxes through electrode reactions, and ionic transport occurs to maintain electrical neutrality. With an electrophoretic effect, various ions move across the skin, each carrying a portion of the current. The contribution of each ion to the total charge transport is defined by its transport number, with the sum of transport numbers for all ions equaling 1. According to Faraday's law, the flux of electrophoresis of each ion is given by:

$$J_{EP} = \frac{t_i \bullet I}{F \bullet Z_i} \tag{2}$$

where t_i is the transport number of ion i, Z_i is the valence of the ith ion, F is Faraday's constant, I is the applied current.

2.1.2. Electroosmotic flow

Electroosmotic flow (EOF) is the primary transport mechanism for uncharged and large molecules. At normal physiological pH, the skin is negatively charged, which makes it selectively permeable to cations [37]. This selective permeability induces an EOF of solvent, which carries neutral molecules from the anode to the cathode. The flow velocity (v_{EO}) is proportional to the potential gradient created by the electric field, described by the equation:

$$v_{EO} = -\frac{\varepsilon \zeta \rho I}{\eta} \tag{3}$$

where I is the current density applied to the fluid conduit. ε is the dielectric constant of the solvent, ζ is the zeta potential of the negative charge fixed in the conduit media, ρ is the specific resistance of the sample, and η is the viscosity of the solvent. The electroosmotic flux contribution to the transport of a solute "j" present in the anodal compartment at a molar concentration c_j can be expressed as:

$$J_{EO} = v_{EO} \bullet c_j \tag{4}$$

The contributions of electrophoresis, electroosmosis, and passive diffusion to the total iontophoretic flux are influenced by the structure and physicochemical properties of the transported species. For small ions or molecules like Na^+ or Cl^-, electrophoresis is the dominant mechanism, while neutral solutes are primarily transported through EOF and passive diffusion.

2.2. Reverse iontophoresis

RI, a subset of IP, is a technique that applies an electric current in the opposite direction to extract ions or small molecules from the skin for diagnostic purposes [34]. This method is primarily used for the non-invasive detection of biomarkers such as glucose, lactate, and other substances found in ISF. The mechanisms of extracting ions or molecules in RI are similar to IP but in reverse, with the flux equations remaining largely the same. For example, small molecules can be drawn out through the electrophoretic effect, where the current interacts with the ions, causing them to migrate to the surface for sampling. Additionally, the applied current can generate an EOF that pulls ISF, along with its dissolved ions, toward the electrode at the skin surface (Fig. 1).

3. Preparation of microneedles

3.1. Materials

The selection of materials for MNs fabrication is crucial to achieving the desired mechanical properties, biocompatibility, and functionality for specific applications. Inorganic non-metallic materials like silicon and ceramics, with its high precision and ability to form intricate structures, are commonly used to create sharp, precise MNs, although it is not biodegradable [38]. Metals like stainless steel, titanium, aluminum and gold are preferred when high strength, durability, and rigidity are required, especially for solid or hollow MNs used in IP-assisted drug delivery [39]. In addition, polymer materials are also employed thanks to their versatility, biocompatibility, and ease of processing. They are particularly suited for creating dissolving MNs, such as those made from polyvinyl alcohol, polylactic acid, and poly (lactic-co-glycolic acid) (PLGA), which dissolve in bodily fluids to release drugs [40–42]. Other polymers like hyaluronic acid, methacrylated hyaluronic acid and poly(glycidyl methacrylate) (PGMA) are utilized to fabricate hydrogel and porous MNs [43–45]. Polymers can also be functionalized by incorporating conductive materials like conductive polymer (poly(3,4-ethylenedioxythiophene) polystyrene sulfonate (PEDOT: PSS), polypyrrole and polyaniline for IP-based sensing and drug delivery [46–49].

3.2. Fabrication techniques

MNs fabrication techniques, including micro-electro-mechanical systems (MEMS), laser cutting or ablation, micro-molding, drawing method and 3D printing, etc., vary widely in terms of precision, material compatibility, and scalability [50]. MEMS, including lithography and etching, are ideal for producing solid MNs from silicon, metal, or polymers, as well as hollow MNs [51,52]. These techniques allow for high precision and scalability, though they require expensive, specialized equipment and are better suited for smaller production batches. Laser-based methods, such as laser drilling and laser ablation, offer flexibility and precision, particularly for creating solid or hollow MNs from a variety of materials like metals and polymers [53,54]. These techniques are fast and well-suited for prototyping but can be costly and slow for large-scale production. Micro-molding, which involves injecting materials like polymers and hydrogels into molds, is ideal for mass-producing dissolving MNs made from biodegradable materials, as well as hydrogel and porous MNs for controlled drug release [55]. Drawing-based methods allow for precise control over MN geometry and are ideal for creating hollow MNs, though they are labor-intensive and limited to glass or metal materials [56]. Finally, 3D printing provides unparalleled design flexibility, enabling the creation of complex MNs from a variety of materials, including hydrogels or hydrogel matrix-based conductive materials [57,58]. This technique is particularly useful for creating hydrogel or dissolving MNs and allows for rapid prototyping.

4. Iontophoresis-assisted microneedles for transdermal biosensing

This section focuses on the synergistic potential of IP-assisted MNs in biosensing applications, highlighting their unique advantages and emerging trends. MNs, typically ranging from hundreds of micrometers to a few millimeters in length, painlessly penetrate the skin's outer layers to access ISF, enabling continuous monitoring of analytes (i.e. glucose, lactate, and physiological parameters, etc.) that are critical for diabetes management and metabolic disorders [33,59]. In RI, one microneedle is usually inserted into the skin as an active electrode to extract biomarkers, with a distant reference electrode completing the circuit. When a low-level electric current is applied, charged analytes migrate towards the microneedle electrodes owing to the RI, where they can be detected and quantified using electrochemical or optical detection methods [34].

4.1. Solid microneedle

The integration of solid MNs with RI for transdermal biosensing leverages the precision of solid MNs to create microchannels (MCs) in the skin, enhancing the efficiency of RI in extracting ISF for analysis. Cheng et al. reported a solid MNs-based touch-actuated device for glucose

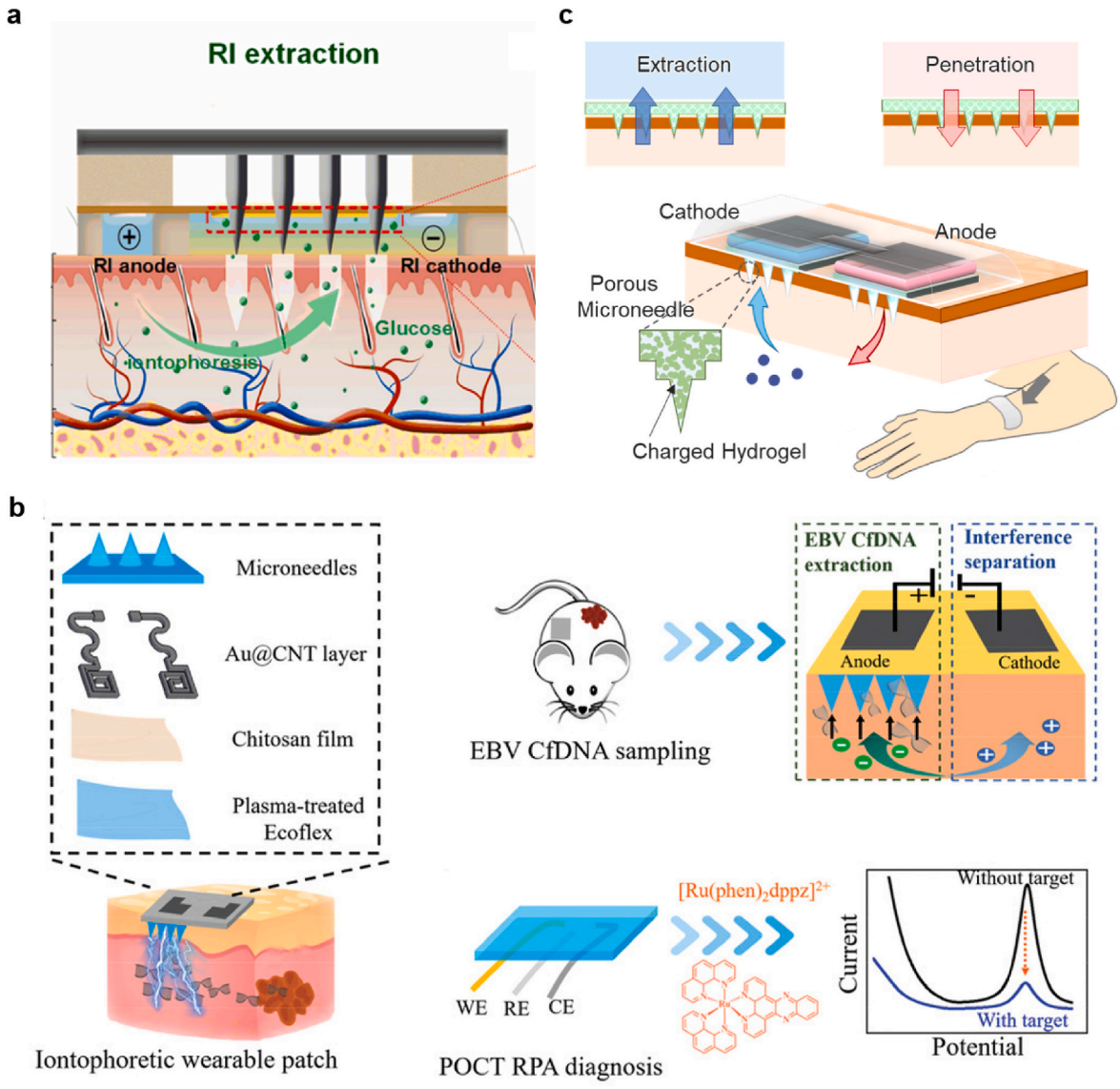

Fig. 3. IP-assisted MNs devices for transdermal biosensing. a) Smartphone-based glucose electrochemical detection platform integrated microneedle array with RI techniques for the minimally invasive detection of glucose in ISF [60]. b) Hydrogel MNs for cell-free DNA capture and sensing [65]. c) Porous MNs generating EOF for glucose sensing [66].

monitoring in ISF (Fig. 3a) [60]. The touch-actuated sensor is composed of solid MNs for skin penetration, the RI unit for ISF extraction and the sensing unit for glucose monitoring. After the penetration of the solid MNs with finger press, a transient microchannel was created, followed by the auto-retraction of the solid MNs due to the elastic property of the porous ring. Since the skin is negatively charged, the neutral glucose was extracted at the cathode compartment driven by the EOF. This wireless sensor achieved an enhanced extraction flux of glucose, which is ca. 1.6 times higher than the RI-only method based on both in vitro and in vivo experiments. Solid MNs can also be incorporated with conductive materials [61–63]. This enhances the MNs' ability to detect electrochemical signals from biomarkers, enabling real-time, non-invasive biosensing with improved sensitivity and response time. For instance, Mokhtar et al. proposed the conductive solid MNs towards electrochemically assisted skin sampling based on a cut-coat method [64]. Two different variants of doped PEDOT are coated on polymethyl methacrylate MNs. Several layers of absorbent paper were then sandwiched in between. With applied potential, more anions moved to the anode and more cationic ions moved to the cathode compartment due to electromigration. The MN skin sampler enables the ions extraction from the skin as a step towards in vivo ISF extraction.

4.2. Hydrogel microneedle

The hydrogel MNs are typically fabricated using a mold-based approach, where a pre-polymer solution is cast into molds and subsequently polymerized [67]. For example, Yang et al. developed a wearable hydrogel MNs patch for ISF cell-free DNA capture and sensing (Fig. 3b) [65]. The hydrogel was made of polymethyl vinyl ether-alt-maleic acid (PMVE/MA), which can absorb the Epstein-Barr virus cell-free DNA in the ISF. Since the DNA has a negative charge, it was extracted from the anode compartment due to the electromigration governed by Faraday's law. To increase capture efficiency, the anode electrode was coated with a positively charged hyaluronic acid to enhance the osmotic pressure from the blood capillary. Owing to the enhanced extraction efficiency assisted by RI and MNs, the proposed wearable device successfully isolates the cell-free DNA target from ISF within 10 min, with a threshold of 5 copies per μL and a maximum capture efficiency of 95.4 %. This combination enables continuous, non-invasive monitoring of biomarkers, making it particularly valuable

for managing chronic conditions like diabetes or for real-time physiological monitoring in healthcare and fitness settings.

4.3. Porous microneedle

The porous structure of the MNs increases the surface area for fluid extraction, while RI ensures a steady and controlled extraction process, leading to more accurate and reliable readings. Unlike hollow MNs, porous MNs avoid clogging issues during fluid extraction, allowing fluid to pass through multiple micro-pores. This method is particularly advantageous for monitoring glucose levels in diabetic patients or tracking other biomolecules, providing a painless alternative to traditional blood sampling. Kusama et al. developed a porous MNs device generating EOF for glucose determination (Fig. 3c) [66]. The charged porous MNs introduce four novel benefits to IP: (1) a reduction in transdermal resistance due to its minimally invasive penetration of the highly resistant stratum corneum; (2) further decreased resistance facilitated by the interconnectivity of micropores; (3) the ability to transport small or larger molecules through interconnected micropores; and (4) the generation of EOF. The EOF produced by the porous MNs significantly enhances glucose transport, achieving approximately 10 times greater efficiency compared to passive diffusion in a Franz cell setup using pig skin as a barrier. Despite the progress mentioned above, integrating IP-assisted MNs for biosensing presents several technical challenges. One major issue is signal interference from the electrical currents used in IP, which can affect the accuracy and reliability of biosensor readings, especially in dynamic physiological conditions. Moreover, the high energy demands of wearable systems pose a significant obstacle. Future advancements should focus on developing efficient, compact, and durable power sources to enhance the portability and practicality of these devices.

5. Iontophoresis-assisted microneedles for transdermal drug delivery

IP-assisted MNs represent a cutting-edge approach for transdermal drug delivery, combining the benefits of minimally invasive MNs with the enhanced transport efficiency of IP [68]. Different from RI where ISF is extracted, IP delivers drugs into the skin with an opposite flow direction. For two-step drug delivery, MNs are first employed to pierce the skin (press and poke), and IP is then applied to drive the drug into the skin through the holes (release). In the one-step method, however, MNs are usually preloaded with drugs and inserted into the skin, and electrodes are placed on the back side of MNs. By enabling precise, controlled, and localized drug administration, IP-assisted MNs hold significant potential for treating various conditions, from chronic diseases to acute medical needs, offering improved therapeutic efficacy and reduced systemic side effects.

5.1. Solid microneedle

IP-assisted solid MNs have emerged as a promising platform for drug delivery applications, offering precise and controlled delivery of therapeutics through the skin. Zheng et al. reported an IP-driven solid MNs patch for the active transdermal delivery of vaccine macromolecules [69]. The transdermal vaccine delivery strategy of the IP-driven MN patch is "press and poke, IP-driven delivery, and immune response". Animal experiments using BALB/c mice showed that this method induces a stronger immune response than traditional intramuscular injection, proving safe and suitable for at-home vaccination. Vora et al. proposed a solid MNs patch combined with IP device for the delivery of methotrexate into healthy and psoriatic skin [70]. A lower resistance and a higher transepidermal water loss for psoriatic skin indicated damaged barrier function, while histology studies indicated epithelial hyperproliferation and elongated rete ridges. A comparable study by Junadi et al. investigated the transdermal delivery of baclofen [71]. In

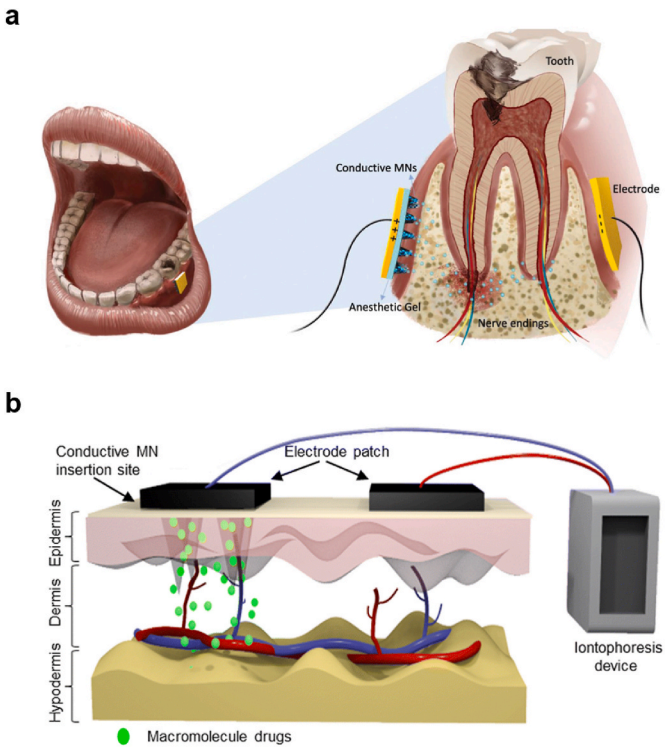

Fig. 4. IP-assisted hydrogel MNs with high conductivity for transdermal drug delivery. a) Conductive hydrogel MNs for local anesthesia (lidocaine) delivery in dentistry [46]. b) IP-assisted conductive hydrogel MNs for the delivery of dextran molecules (3–5 kDa, 150 kDa, and 500 kDa) [47].

vitro permeation experiments were performed using dermatome-processed porcine ear skin in vertical Franz diffusion cells to assess baclofen delivery. Anodal IP was applied at a current density of 0.5 mA/cm^2, with baclofen solutions at pH 4.5 and pH 7.4. In addition, Feng et al. combined solid MNs with the IP technique to facilitate the transdermal delivery and brain distribution of tetramethylpyrazine [72]. Their findings revealed that the MN-IP group significantly reduced the brain infarction area and IL-β expression in middle cerebral artery occlusion rats compared to the control group ($p < 0.05$).

5.2. Hollow microneedle

IP-assisted hollow MNs offer several advantages over traditional drug delivery methods. Detamornrat et al. developed an iontophoretic hollow MNs array system designed for delivering charged molecules and macromolecules, such as proteins [73]. An ex vivo drug permeation study was conducted using a Franz diffusion cell, demonstrating significant increases in permeation rates for various compounds: methylene blue (61-fold), fluorescein sodium (43-fold), lidocaine hydrochloride (54-fold), and BSA-Fluorescein isothiocyanate (FITC) (17-fold) under a current density of 1 mA/cm^2 over 6 h. Additionally, the total amount of drug delivered, comprising both skin retention and receptor compartment levels, was analyzed to distinguish the delivery profiles of different molecules. On the other hand, Arshad et al. developed an IP-coupled hollow MNs approach for the improved transdermal delivery of rabies vaccine [74]. The device shows effective skin penetration, stability, and ~206 % higher immunoglobulin G titers in dogs than MNs alone. This MNs-IP combination also increased rabies virus neutralizing antibodies titers by ~2.2 times, highlighting its potential for transcutaneous vaccine delivery.

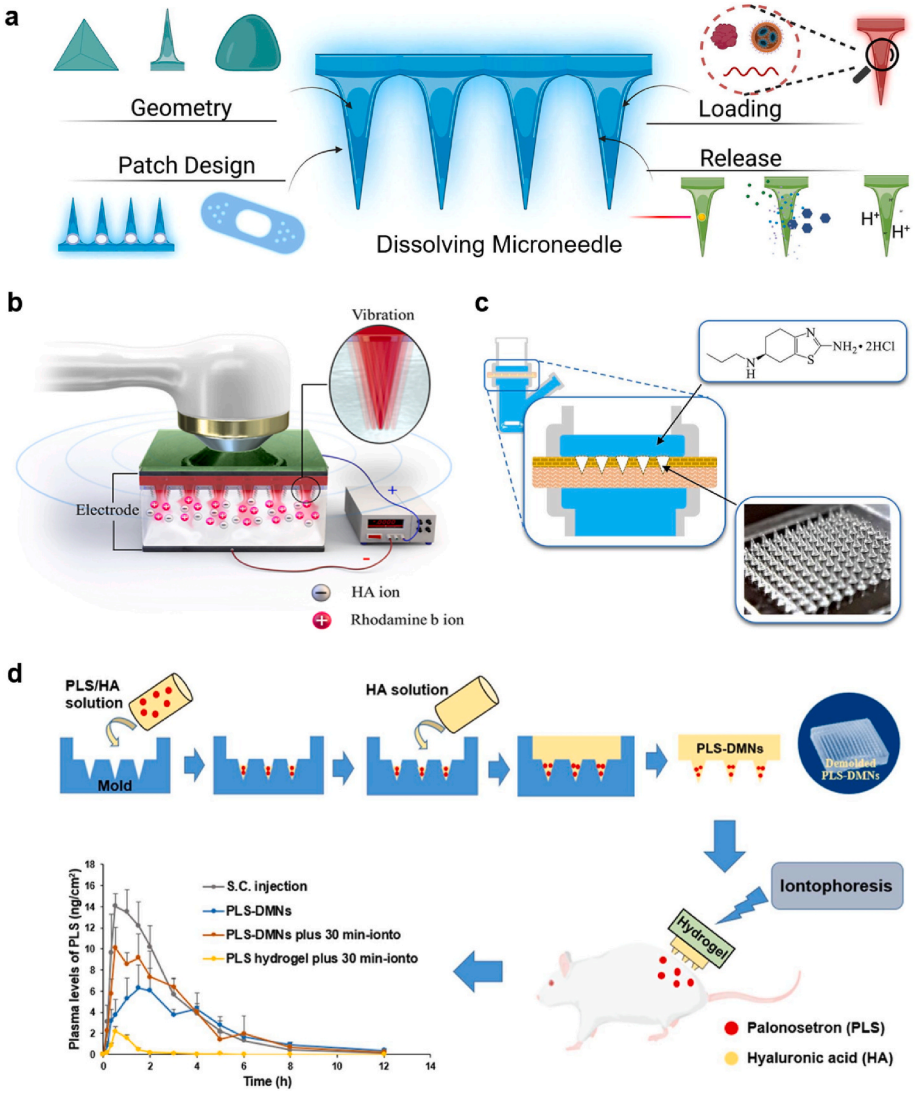

Fig. 5. IP-assisted dissolving MNs for transdermal drug delivery. a) Schematic illustration of dissolving MNs for drug delivery applications [80]. b) Ultrasonically and iontophoretically enhanced dissolving MNs made of hyaluronic acid, with successful releasing of rhodamine [83]. c) MNs create skin MCs for enhanced transdermal delivery of PXCl based on "poke-and-patch" and "poke-and-release" [84]. d) Bolus administration of PLS via skin using dissolving MNs of PLS-DMNs [85].

5.3. Hydrogel microneedle

Hydrogel MNs equipped with conductive elements, such as electrodes or conductive materials like polypyrrole and poly(3,4-ethylenedioxythiophene) (PEDOT), facilitate the flow of electric current and enhance drug penetration. The integration of IP with conductive hydrogel MNs enables precise control over drug delivery parameters, including dosage and release kinetics. By modulating the intensity and duration of the applied electric current, one can tailor treatment regimens to individual patient needs. For example, Donnelly et al. proposed a hydrogel MNs containing 15 % w/w poly(methylvinylether/maelic acid) (PMVE/MA) and 7.5 % w/w poly(ethyleneglycol) and coupled with IP technique. The results showed that the combination of integrated hydrogel MN and IP led to a significantly accelerated BSA-FITC permeation [75]. Xu's group developed a hyaluronic acid-based conductive hydrogel MNs enhanced by IP for painless dental anesthesia (Fig. 4a) [46]. The hydrogel MNs array creates micro-conduits that lower the resistance of the oral mucosa. This reduced tissue resistance facilitates the application of a low-voltage current, enabling more efficient and targeted delivery of drug molecules to the sensory nerves supplying the teeth. Additionally, a hydrogel MN system capable of delivering macromolecules was developed (Fig. 4b) [47]. This study reported a conductive hydrogel MNs using polyaniline and hyaluronic acid, combined with IP to enhance the delivery of dextran macromolecules. The system demonstrated improved penetration of dextran molecules (3–5 kDa, 150 kDa, and 500 kDa) to a depth of approximately 1536 μm in an agarose gel model. Peng et al. proposed an IP-integrated hydrogel MNs by incorporating the carbon nanotubes with boronate-containing hydrogel, offering on-demand insulin delivery with minimal invasion [76].

5.4. Dissolving microneedle

Dissolving MNs represents a cutting-edge approach to drug delivery with a user-friendly interface and minimal patient discomfort [77–81]. Dissolving MNs are fabricated from biocompatible polymers that encapsulate drug payloads. These MNs are designed to painlessly penetrate the skin's outer layers and subsequently dissolve, releasing the encapsulated drugs into the underlying tissue (Fig. 5a). The integration of IP enhances drug delivery by facilitating the transport of charged drug molecules through the skin barriers. For example, Abbasi et al. developed a dissolving MNs for browning subcutaneous adipose tissue by combining it with IP technique [82]. The results show that this method enhances white adipose tissue (WAT) browning, leading to increased

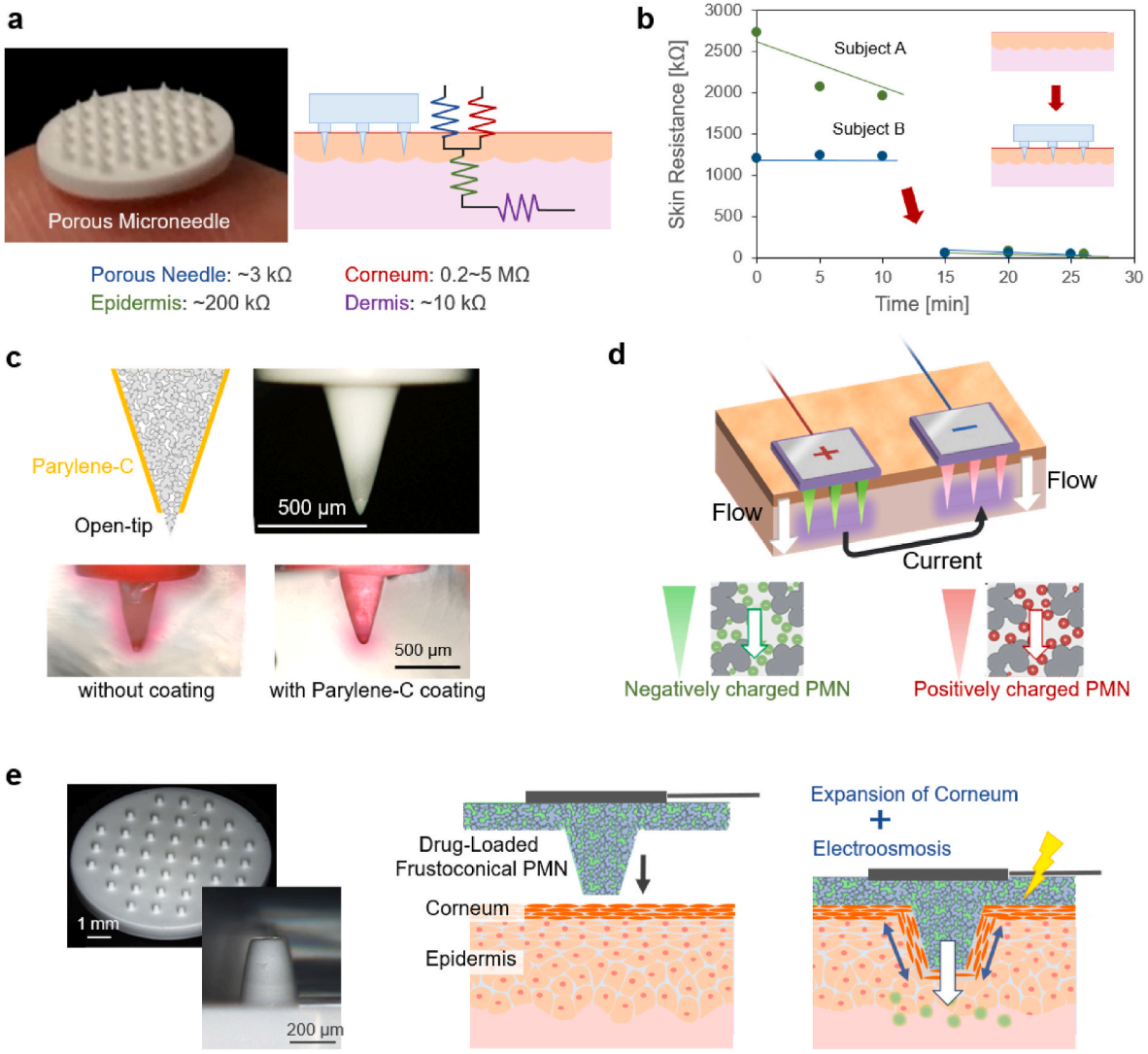

Fig. 6. IP-assisted porous MNs for transdermal drug delivery. a) Structure of porous MNs and the illustration of equivalent DC circuits of different skin layers [66]. b) The DC resistance of human arms before and after porous MNs administration. c) Open-tip MNs with parylene-C coating [94]. d) Dual-mode drug delivery by aligning the directions of EOF [95]. e) Non-invasive frustoconical porous MNs enables the synergy of the expansion of the stratum corneum and EOF promotion for transdermal administration [96].

energy expenditure, reduced body weight, and improved metabolic outcomes. Bok et al. reported an ultrasonically and iontophoretically enhanced drug delivery system based on dissolving MNs patches (Fig. 5b) [83]. This study presents a multifunctional transdermal delivery system using hyaluronic acid MNs. By controlling the concentration of the hyaluronic acid solution, the MNs can regulate drug filling. The system utilizes ultrasonication to dissolve MNs and AC iontophoresis to improve drug diffusion. The results demonstrate that this combined approach significantly increases permeation and reduces delivery time compared to passive methods, paving the way for effective macromolecular drug delivery based on response time. Saepang et al. explores the use of MNs to create skin MCs for enhanced transdermal delivery of pramipexole dihydrochloride (PXCl) (Fig. 5c) [84]. In vitro experiments using human skin compared different delivery methods, including "poke-and-patch" and "poke-and-release," with drug-loaded dissolving MNs and hydrogel-forming MNs (HGMN). The dissolving MNs patches significantly improved PXCl delivery compared to conventional methods, while HGMN patches provided a more sustained release over 72 h. Fig. 5d shows the feasibility of the bolus administration of palonosetron (PLS) via skin using dissolving MNs of palonosetron hydrochloride (PLS-DMNs) [85]. Made with sodium hyaluronate, PLS-DMNs delivered 83.2 % of the drug in 5 min. In vitro study showed significantly higher PLS permeation than passive methods. In vivo studies in rats indicated that the area under the curve and the time to reach the peak after PLS-DMNs were comparable to subcutaneous injections. These results suggest that PLS-DMNs with IP offer a painless, rapid alternative for PLS delivery. Other applications like the transdermal delivery of sumatriptan succinate have also been reported [86]. Overall, IP-assisted dissolving MNs represent a significant advancement in drug delivery, offering precise and controlled administration of therapeutics with minimal invasiveness.

5.5. *Porous microneedle*

Porous MNs feature an array of microscale pores distributed across their surface, allowing for the controlled release of therapeutic agents into the skin [87,88]. The porous structure of the MNs then facilitates the diffusion of drugs into the skin, where they can exert their therapeutic effects. Simultaneously, the application of an electric current via IP promotes the migration of charged drug molecules toward the target site, enhancing the overall delivery efficiency. The porosity and pore size of the MNs can be tailored to control the release kinetics of drugs

Table 1
Summary of applications for iontophoretic MNs-based drug delivery.

Type of MNs	Fabrication Technique	Applications			Performance	Mechanisms	Restrictions	Key References
		Small-molecule drugs	Macromolecules	Vaccines				
Solid MNs assembled with Ag/AgCl electrodes	Micromachining from stainless steel 316 L			Vaccine: Ovalbumin (44.5 kDa)	1.58 μg/min under 0.5 mA/cm^2	"Press and poke, IP-driven delivery"	Complex manufacturing; Low biocompatibility	[69]
Maltose MNs	Micro-mold casting	Small-molecule drugs: Baclofen (214 Da)			45.51 ± 0.76 μg/cm^2	"Press and poke, IP-driven delivery"	Low mechanical strength; Reduced efficiency due to the self-healing of skin	[71]
Polymeric hollow MNs	Micromachining from polyether ether ketone (PEEK) sheets	Small-molecule drugs: methylene blue (319.85 Da), fluorescein sodium (376.3 Da) and lidocaine hydrochloride (270.8 Da)	Macromolecules: BSA-FITC (66 kDa)		728.6 ± 108.6 μg; 1384.6 ± 269.3 μg; 1513.7 ± 234.8 μg; 370.1 ± 31.2 μg. under 1 mA/cm^2 for 6 h	Electrophoretic delivery (positively charged drug is loaded at the anode and negatively charged drug is loaded at the cathode)	Limited for certain charged molecules; Risk of clogging	[73]
Conductive hydrogel MNs	Micro-mold casting	Small-molecule drugs: Lidocaine (234 Da)			96.3 ± 6.4 % under 3 mA/cm^2	Electrophoretic delivery	Limited for certain charged molecules; Risk of electrical stimulation	[46]
PLGA dissolving MNs	Micro-mold casting	Small-molecule drugs: Metformin (129.2 Da)			81 μg of metformin was delivered within 8 h under 0.2 mA/cm^2	Electrophoretic delivery	Limited for certain charged molecules; Limited drug loading capacity	[82]
Hyaluronic acid (HA) dissolving MNs	Micro-mold casting	Small-molecule drugs: Rhodamine B (479 Da)			1.1 ng/cm^{2}s under 10 Hz and 10 V	Ultrasound and Electrophoretic delivery	Low mechanical strength; Risk of electrical stimulation	[83]
PGMA porous MNs	Solvent casting and particulate leaching	Small-molecule drugs: Rhodamine B (479 Da);	Macromolecules: FITC–dextran (10 and 40 kDa);	Vaccine: Ovalbumin (44.5 kDa)	0.11 μg/min for RhB; 0.096 μg/min for 10 kDa FITC-dextran; 0.058 μg/min for 40 kDa FITC-dextran under 0.5 mA/cm^2	EOF	Risk of electrical stimulation; Low durability due to the concentration polarization	[95]

and optimize therapeutic efficacy. Smaller pore sizes enable sustained release over an extended period, while larger pores facilitate rapid drug diffusion for immediate effects. Li et al. demonstrated an IP-driven porous MNs array patch (IDPMAP) for active transdermal drug delivery [89]. IDPMAP integrates porous MA with IP into a single transdermal patch, thus realizing the one-step drug administration strategy of "penetration, diffusion, and IP." On the other hand, Wang et al. reported a hydrogel-based porous MNs for the cancer therapy [90]. However, those methods are all based on the electrophoretic mechanism, limiting the selection of drugs. Nishizawa group has proposed PGMA porous MNs based on the particulate leaching method (Fig. 6a) [45,91]. This porous MNs have been advanced for transdermal drug delivery using EOF, thereby expanding the range of drug candidates and improving the delivery efficiency [66,92,93]. The administration of porous MNs can significantly lower the transdermal resistance of stratum corneum with low invasive penetration, thereby achieving a higher delivery efficiency (Fig. 6b). Moreover, to improve delivery efficiency, an open-tip porous MNs with parylene-C coating was developed (Fig. 6c) [94]. The open-tip porous MNs guides the flow of solvent with the drug focusing on the tip and minimizing the flow from the substrate and side parts. Furthermore, Wang et al. developed a dual-mode delivery profile by reversing the direction of EOF in the cathode compartment (Fig. 6d) [95]. However, conventional sharp needles still exhibit invasive properties to human beings. A frustoconical porous MNs for electroosmotic transdermal drug delivery was developed (Fig. 6e) [96]. Additionally, the integration of porous MNs with other actuators has been proposed, demonstrating its versatile property for transdermal drug delivery applications [97]. In conclusion, IP-assisted porous MNs offer a promising approach for enhanced drug delivery, combining the advantages of MNs technology with the controlled release facilitated by IP. Table 1 summarizes various applications of MNs combined with IP.

6. Integrated closed-loop system

The integration of IP-assisted MNs has garnered significant interest in their potential to enable closed-loop systems capable of simultaneous biosensing and drug delivery. One of the key advantages of IP-assisted MNs in closed-loop systems is their ability to provide immediate feedback through real-time biosensing [98]. By continuously monitoring biomarkers such as glucose, lactate, or specific drug concentrations in ISF, these devices can dynamically adjust drug delivery profiles. The integration of biosensing and drug delivery functions within a single platform offers several benefits, including enhanced therapeutic efficacy, reduced side effects, and improved patient compliance. For example, in diabetes management, closed-loop systems can maintain tight glycemic control by adjusting insulin delivery based on real-time glucose measurements, thereby minimizing the risk of hypoglycemia or hyperglycemia [99–103]. Yang et al. introduced a biomimetic solid MNs theranostic platform designed for intelligent and precise diabetes management (Fig. 7a) [104]. The MNTP integrates a miniaturized

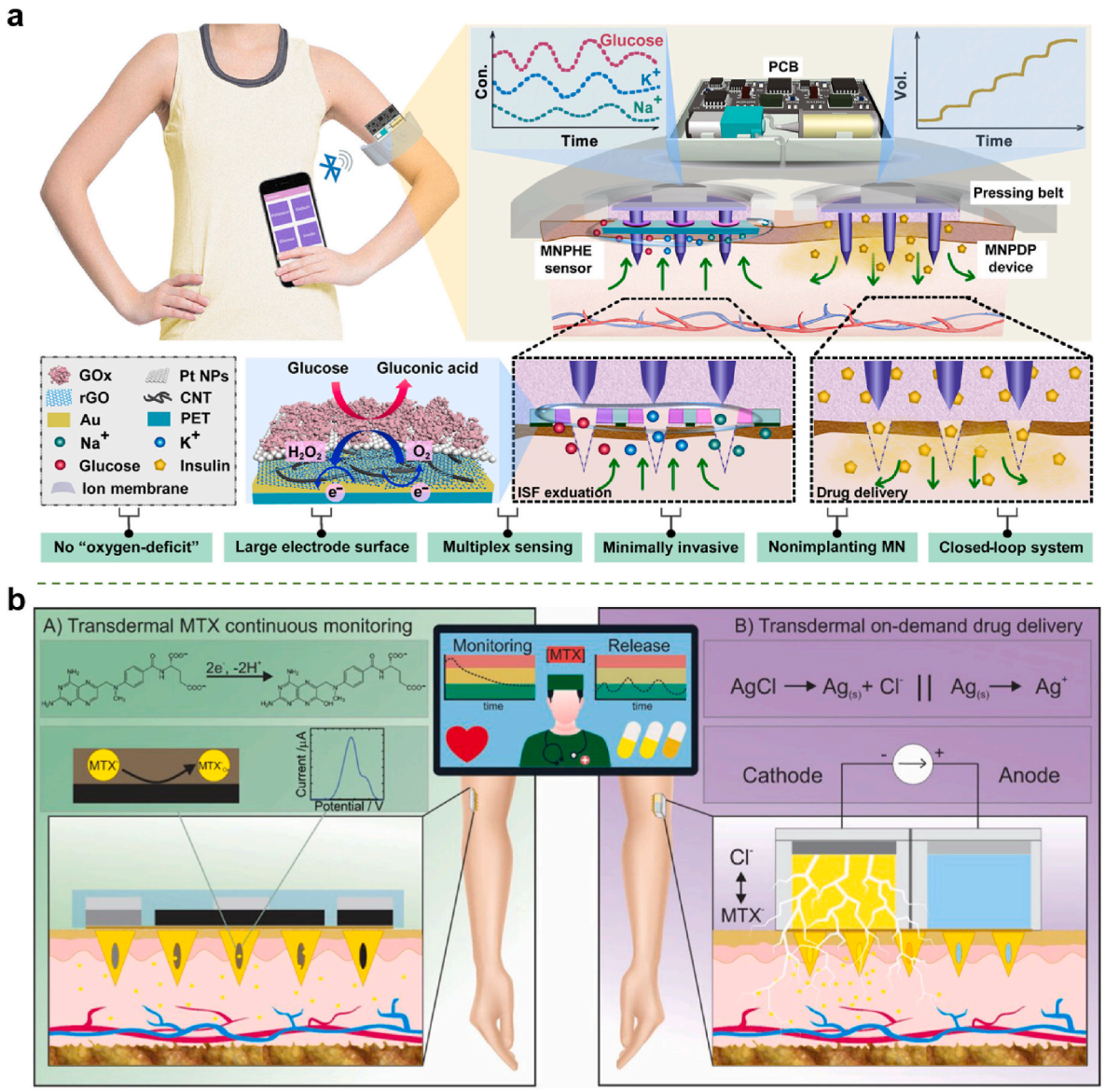

Fig. 7. Integrated closed-loop system. a) Biomimetic solid MNs theranostic platform for intelligent and precise management of diabetes [104]. b) A wearable hollow MNs-based array patch for continuous electrochemical monitoring and drug delivery [105].

circuit and MNs arrays for on-demand skin penetration, facilitating ISF extraction for the simultaneous detection of glucose and physiological ions, as well as subcutaneous insulin delivery. In addition to diabetes management, Parrilla et al. reported a wearable hollow MNs-based array of patches for rheumatoid arthritis treatment (Fig. 7b) [105]. The hollow MNs array patch is enhanced with conductive pastes and functionalized with cross-linked chitosan to create an MN-based voltammetric sensor for continuous methotrexate (MTX) monitoring. Notably, the chitosan coating prevents biofouling while facilitating the adsorption of MTX on the electrode surface, enabling highly sensitive analysis. Other applications including diabetes-related diseases like chronic wounds were also developed [106]. While the considerable promise of IP-assisted MNs in closed-loop systems, several critical technical bottlenecks must be addressed for practical implementation. One major challenge is optimizing device design to ensure both reliable biosensing and drug delivery over extended periods. To improve long-term performance, advances in materials and miniaturization are needed to balance device durability with precision. Moreover, ensuring accurate and interference-free feedback loops is essential for real-time drug delivery adjustments. Signal interference from environmental noise or electrochemical reactions can compromise the precision of biosensing, requiring more robust noise reduction and filtering techniques to maintain signal integrity. In addition, these devices must be continuously powered while remaining compact and comfortable. Progress in energy harvesting, low-power electronics, and efficient power management systems is crucial to address this limitation. Finally, regulatory and clinical validation remain major obstacles to the widespread adoption of closed-loop systems. Rigorous testing through clinical trials is necessary to ensure these systems meet medical standards.

7. Conclusion and perspectives

As our understanding of IP-assisted MNs advances, their potential applications continue to expand, offering transformative opportunities in diagnostics and therapy. However, integrating IP with MNs also introduces specific challenges. Solid MNs, for instance, need further optimization to ensure effective electric current distribution and improve biocompatibility, requiring the materials advancement that promote uniform current flow and enhance skin penetration. For hollow MNs, challenges like clogging and structural fragility under

iontophoretic conditions should be addressed, with future research focusing on improving material robustness and incorporating anti-clogging techniques. Dissolvable MNs, although promising for biodegradable and sustained drug release, face issues related to conductivity and controlled releasing rates, necessitating innovations in biodegradable conductive polymers or hydrogels. Importantly, the integration of IP-MNs into closed-loop systems presents hurdles such as ensuring a reliable power supply and seamless interaction between sensing and drug delivery components. Research should explore energy-efficient microelectronics, power harvesting technologies, and advanced circuit designs to create practical, wearable systems. Incorporating artificial intelligence and machine learning could also enhance these systems, enabling adaptive responses based on real-time sensing. By focusing on these specific challenges, future research can help unlock the full potential of this technology, offering precise, accessible, and minimally invasive solutions for diagnostics and therapy, ultimately advancing personalized healthcare and improving patient outcomes.

CRediT authorship contribution statement

Gaobo Wang: Writing – review & editing, Writing – original draft, Conceptualization. **Natsuho Moriyama:** Writing – original draft. **Soichiro Tottori:** Writing – original draft. **Matsuhiko Nishizawa:** Writing – review & editing, Supervision.

Declaration of competing interest

The authors declare that they have no known competing financial interests or personal relationships that could have appeared to influence the work reported in this paper.

Acknowledgments

This work was partly supported by Grant-in-Aids for Scientific Research S (22H04956) from the Ministry of Education, Culture, Sports, Science and Technology, Japan.

Data availability

No data was used for the research described in the article.

References

[1] M. Starace, S. Cedirian, F. Quadrelli, B.M. Piraccini, Iontophoresis as a potential treatment for alopecia areata incognita, Int. J. Dermatol. Venereol. 159 (2024) 201–202, https://doi.org/10.23736/S2784-8671.24.07723-5.
[2] S. Eslami, F. Tahmasbi, A. Rahimi-Mamaghani, S. Sanaie, C. Bettocchi, O. Sedigh, F. Soleimanzadeh, Investigating iontophoresis as a therapeutic approach for Peyronie's disease: a systematic review, Sex Med. Rev. qeae058 (2024), https://doi.org/10.1093/sxmrev/qeae058.
[3] R. Ragit, P. Fulzele, N.V. Rathi, N.R. Thosar, M. Khubchandani, N.S. Malviya, S. R. Das, Iontophoresis as an effective drug delivery system in dentistry: a review, Cureus. J. Med. Sci. 14 (2022) e30658, https://doi.org/10.7759/cureus.30658.
[4] M. Lombardo, V. Villari, N. Micali, P. Roy, S.H. Sousa, G. Lombardo, Assessment of trans-scleral iontophoresis delivery of lutein to the human retina, J. Biophotonics 11 (2018) e201700095, https://doi.org/10.1002/jbio.201700095.
[5] P.L. Langley, Iontophoresis to aid in releasing tendon adhesions. Suggestion from the field, Phys. Ther. 64 (1984) 1395, https://doi.org/10.1093/ptj/64.9.1395.
[6] M.J. Pikal, The role of electroosmotic flow in transdermal iontophoresis, Adv. Drug Deliver. Rev. 9 (1992) 201–237, https://doi.org/10.1016/0169-409x(92)90024-K.
[7] V. Merino, A. Lopez, D. Hochstrasser, R.H. Guy, Noninvasive sampling of phenylalanine by reverse iontophoresis, J. Contr. Release 61 (1999) 65–69, https://doi.org/10.1016/s0168-3659(99)00102-9.
[8] G. Rao, R.H. Guy, P. Glikfeld, W.R. LaCourse, L. Leung, J. Tamada, R.O. Potts, N. Azimi, Reverse iontophoresis: noninvasive glucose monitoring in vivo in humans, Pharm. Res. 12 (1995) 1869–1873, https://doi.org/10.1023/a:1016271301814.
[9] G. Rao, P. Glikfeld, R.H. Guy, Reverse iontophoresis: development of a noninvasive approach for glucose monitoring, Pharm. Res. 10 (1993) 1751–1755, https://doi.org/10.1023/a:1018926215306.
[10] M. Akimoto, K. Maeda, M. Hata, S. Bohman, S. Nakano, T. Omi, Y. Hayatsu, Optimum conditions of iontophoresis and electroporation in the transdermal drug delivery in aesthetic dermatology, J. Am. Acad. Dermatol. 70 (2014) AB32, https://doi.org/10.1016/j.jaad.2014.01.135.
[11] J.B. Sloan, K. Soltani, Iontophoresis in dermatology, J. Am. Acad. Dermatol. 15 (1986) 671–684, https://doi.org/10.1016/S0190-9622(86)70223-5.
[12] R. Lambrecht, R. Clijsen, J. Taeymans, A. Clarys, A.O. Barel, Iontophoresis in physical therapy - fact or fiction, Sportverletz. Sportsc. 17 (2003) 159–164.
[13] F. Henriquez, D. Celentano, M. Vega, G. Pincheira, J.O. Morales-Ferreiro, Modeling of microneedle arrays in transdermal drug delivery applications, Pharmaceutics 15 (2023) 358, https://doi.org/10.3390/pharmaceutics15020358.
[14] C.J.W. Bolton, O. Howells, G.J. Blayney, P.F. Eng, J.C. Birchall, B. Gualeni, K. Roberts, H. Ashrafa, O.J. Guy, Hollow silicon microneedle fabrication using advanced plasma etch technologies for applications in transdermal drug delivery, Lab Chip 20 (2020) 2788–2795, https://doi.org/10.1039/d0lc00567c.
[15] K. Kusamori, H. Katsumi, R. Sakai, R. Hayashi, Y. Hirai, Y. Tanaka, K. Hitomi, Y. Quan, F. Kamiyama, K. Yamada, S. Sumida, K. Kishi, K. Hashiba, T. Sakane, A. Yamamoto, Development of a drug-coated microneedle array and its application for transdermal delivery of interferon alpha, Biofabrication 8 (2016) 015006, https://doi.org/10.1088/1758-5090/8/1/015006.
[16] S. Liu, M. Jin, Y. Quan, F. Kamiyama, H. Katsumi, T. Sakane, A. Yamamoto, The development and characteristics of novel microneedle arrays fabricated from hyaluronic acid, and their application in the transdermal delivery of insulin, J. Contr. Release 161 (2012) 933–941, https://doi.org/10.1016/j.jconrel.2012.05.030.
[17] S.Y. Ruan, Y.T. Zhang, N.P. Feng, Microneedle-mediated transdermal nanodelivery systems: a review, Biomater. Sci. 9 (2021) 8065–8089, https://doi.org/10.1039/d1bm01249e.
[18] F. Tasca, C. Tortolini, P. Bollella, R. Antiochia, Microneedle-based electrochemical devices for transdermal biosensing: a review, Curr. Opin. Electrochem. 16 (2019) 42–49, https://doi.org/10.1016/j.coelec.2019.04.003.
[19] J. Li, M. Wei, B. Gao, A review of recent advances in microneedle-based sensing within the dermal ISF that could transform medical testing, ACS Sens. 9 (2024) 1149–1161, https://doi.org/10.1021/acssensors.4c00142.
[20] A.F. Moreira, C.F. Rodrigues, T.A. Jacinto, S.P. Miguel, E.C. Costa, I.J. Correia, Microneedle-based delivery devices for cancer therapy: a review, Pharmacol. Res. 148 (2019) 104438, https://doi.org/10.1016/j.phrs.2019.104438.
[21] G. Ma, C. Wu, Microneedle, bio-microneedle and bio-inspired microneedle: a review, J. Contr. Release 251 (2017) 11–23, https://doi.org/10.1016/j.jconrel.2017.02.011.
[22] H.Y. Sun, Y.B. Zheng, G.Y. Shi, H. Haick, M. Zhang, Wearable clinic: from microneedle-based sensors to next-generation healthcare platforms, Small 19 (2023) 2207539, https://doi.org/10.1002/smll.202207539.
[23] Q. Zhou, K. Dong, M. Wei, B. He, B. Gao, Rolling stone gathers moss: rolling microneedles generate meta microfluidic microneedles (MMM), Adv. Func. Mater. 34 (2024) 2316565, https://doi.org/10.1002/adfm.202316565.
[24] J. Bai, D. Liu, X. Tian, Y. Wang, B. Cui, Y. Yang, S. Dai, W. Lin, J. Zhu, J. Wang, A. Xu, Z. Gu, S. Zhang, Coin-sized, fully integrated, and minimally invasive continuous glucose monitoring system based on organic electrochemical transistors, Sci. Adv. 10 (2024) eadl1856, https://doi.org/10.1126/sciadv.adl1856.
[25] R. Zhang, Q. Miao, D. Deng, J.X. Wu, Y.Q. Miao, Y. Li, Research progress of advanced microneedle drug delivery system and its application in biomedicine, Colloid Surf. B: Biointerfaces. 226 (2023) 113302, https://doi.org/10.1016/j.colsurfb.2023.113302.
[26] A.M. Helmy, Overview of recent advancements in the iontophoretic drug delivery to various tissues and organs, J. Drug Deliv. Sci. Tec. 61 (2021) 102332, https://doi.org/10.1016/j.jddst.2021.102332.
[27] T.K. Giri, S. Chakrabarty, B. Ghosh, Transdermal reverse iontophoresis: a novel technique for therapeutic drug monitoring, J. Contr. Release 246 (2017) 30–38, https://doi.org/10.1016/j.jconrel.2016.12.007.
[28] R.H. Guy, Y.N. Kalia, M. Begoña Delgado-Charro, V. Merino, A. López, D. Marro, Iontophoresis: electrorepulsion and electroosmosis, J. Contr. Release 64 (2000) 129–132, https://doi.org/10.1016/S0168-3659(99)00132-7.
[29] J. Wang, Z. Lu, R. Cai, H. Zheng, J. Yu, Y. Zhang, Z. Gu, Microneedle-based transdermal detection and sensing devices, Lab Chip 23 (2023) 869–887, https://doi.org/10.1039/D2LC00790H.
[30] M. Zheng, T. Sheng, J. Yu, Z. Gu, C. Xu, Microneedle biomedical devices, Nat. Rev. Bioeng. 2 (2024) 324–342, https://doi.org/10.1038/s44222-023-00141-6.
[31] Y. Zhang, C. Yang, H. Shi, C. Xu, Current technological trends in transdermal biosensing, Adv. NanoBiomed. Res. 2 (2022) 2200040, https://doi.org/10.1002/anbr.202200040.
[32] K.M. Saifullah, Z.F. Rad, Sampling dermal interstitial fluid using microneedles: a review of recent developments in sampling methods and microneedle-based biosensors, Adv. Mater. Interfaces 10 (2023) 2201763, https://doi.org/10.1002/admi.202201763.
[33] Y. Wang, Y. Wu, Y. Lei, Microneedle-based glucose monitoring: a review from sampling methods to wearable biosensors, Biomater. Sci. 11 (2023) 5727–5757, https://doi.org/10.1039/d3bm00409k.
[34] H. Zheng, Z.H. Pu, H. Wu, C.C. Li, X.G. Zhang, D.C. Li, Reverse iontophoresis with the development of flexible electronics: a review, Biosens. Bioelectron. 223 (2023) 115036, https://doi.org/10.1016/j.bios.2022.115036.
[35] J. Zhang, J. Xu, J. Lim, J.K. Nolan, H. Lee, C.H. Lee, Wearable glucose monitoring and implantable drug delivery systems for diabetes management, Adv. Healthc. Mater. 10 (2021) 2100194, https://doi.org/10.1002/adhm.202100194.

[36] A. Sieg, V. Wascotte, Diagnostic and therapeutic applications of iontophoresis, J. Drug Target. 17 (2009) 690–700, https://doi.org/10.3109/10611860903089750.
[37] M.J. Pikal, The role of electroosmotic flow in transdermal iontophoresis, Adv. Drug Deliv. Rev. 46 (2001) 281–305, https://doi.org/10.1016/s0169-409x(00)00138-1.
[38] X. Luo, L. Yang, Y. Cui, Microneedles: materials, fabrication, and biomedical applications, Biomed. Microdevices 25 (2023) 20, https://doi.org/10.1007/s10544-023-00658-y.
[39] Y. Zheng, R. Ye, X. Gong, J. Yang, B. Liu, Y. Xu, G. Nie, X. Xie, L. Jiang, Iontophoresis-driven microneedle patch for the active transdermal delivery of vaccine macromolecules, Microsyst. Nanoeng. 9 (2023) 35, https://doi.org/10.1038/s41378-023-00515-1.
[40] J.H. Park, M.G. Allen, M.R. Prausnitz, Biodegradable polymer microneedles: fabrication, mechanics and transdermal drug delivery, J. Contr. Release 104 (2005) 51–66, https://doi.org/10.1016/j.jconrel.2005.02.002.
[41] M.G. McGrath, S. Vucen, A. Vrdoljak, A. Kelly, C. O'Mahony, A.M. Crean, A. Moore, Production of dissolvable microneedles using an atomised spray process: effect of microneedle composition on skin penetration, Eur. J. Pharm. Biopharm. 86 (2014) 200–211, https://doi.org/10.1016/j.ejpb.2013.04.023.
[42] M.A. Luzuriaga, D.R. Berry, J.C. Reagan, R.A. Smaldone, J.J. Gassensmitha, Biodegradable 3D printed polymer microneedles for transdermal drug delivery, Lab Chip 18 (2018) 1223–1230, https://doi.org/10.1039/C8LC00098K.
[43] J. Chudzińska, A. Wawrzyńczak, A. Feliczak-Guzik, Microneedles based on a biodegradable polymer—hyaluronic acid, Polymers 16 (2024) 1396, https://doi.org/10.3390/polym16101396.
[44] G. Wang, Y. Zhang, H. Kwong, M. Zheng, J. Wu, C. Cui, W.Y. Chan, C. Xu, T. H. Chen, On-site melanoma diagnosis utilizing a swellable microneedle-assisted skin interstitial fluid sampling and a microfluidic particle dam for visual quantification of S100A1, Adv. Sci. 11 (2024) 2306188, https://doi.org/10.1002/advs.202306188.
[45] L. Liu, H. Kai, K. Nagamine, Y. Ogawa, M. Nishizawa, Porous polymer microneedles with interconnecting microchannels for rapid fluid transport, RSC Adv. 6 (2016) 48630–48635, https://doi.org/10.1039/c6ra07882f.
[46] R.Z. Seeni, M. Zheng, D.C.S. Lio, C. Wiraja, M.F.B.M. Yusoff, W.T.Y. Koh, Y. Liu, B.T. Goh, C. Xu, Targeted delivery of anesthetic agents to bone tissues using conductive microneedles enhanced iontophoresis for painless dental anesthesia, Adv. Funct. Mater. 31 (2021) 2105686, https://doi.org/10.1002/adfm.202105686.
[47] T. Hu, Z. Zhang, C. Xu, Transdermal delivery of dextran using conductive microneedles assisted by iontophoresis, J. Mater. Chem. B 10 (2022) 8075–8081, https://doi.org/10.1039/d2tb01049f.
[48] Y. Yang, B. Chen, X. Zhang, H. Zheng, Z. Li, C. Zhang, X. Guo, Conductive microneedle patch with electricity-triggered drug release performance for atopic dermatitis treatment, ACS Appl. Mater. Inter. 14 (2022) 31645–31654, https://doi.org/10.1021/acsami.2c05952.
[49] S.M. Mugo, W. Lu, M. Wood, S. Lemieux, Wearable microneedle dual electrochemical sensor for simultaneous pH and cortisol detection in sweat, Electrochem Sci. Adv. 2 (2022) e2100039, https://doi.org/10.1002/elsa.202100039.
[50] S. Lyu, Z. Dong, X. Xu, H.P. Bei, H.Y. Yuen, C.W.J. Cheung, M.S. Wong, Y. He, X. Zhao, Going below and beyond the surface: microneedle structure, materials, drugs, fabrication, and applications for wound healing and tissue regeneration, Bioact. Mater. 27 (2023) 303–326, https://doi.org/10.1016/j.bioactmat.2023.04.003.
[51] A. Tucak, M. Sirbubalo, L. Hindija, O. Rahić, J. Hadžiabdić, K. Muhamedagić, A. Čekić, E. Vranić, Microneedles: characteristics, materials, production methods and commercial development, Micromachines 11 (2020) 961, https://doi.org/10.3390/mi11110961.
[52] C. O'Mahony, R. Sebastian, F. Tjulkins, D. Whelan, A. Bocchino, Y. Hu, J. O'Brien, J. Scully, M. Hegarty, A. Blake, I. Slimi, A.J.P. Clover, A. Lyness, A.M. Kelleher, Hollow silicon microneedles, fabricated using combined wet and dry etching techniques, for transdermal delivery and diagnostics, Int. J. Pharm. 637 (2023) 122888, https://doi.org/10.1016/j.ijpharm.2023.122888.
[53] M.K. Ahmed, M.E. El-Naggar, A. Aldalbahi, M.H. El-Newehy, A.A. Menazea, Methylene blue degradation under visible light of metallic nanoparticles scattered into graphene oxide using laser ablation technique in aqueous solutions, J. Mol. Liq. 315 (2020) 113794, https://doi.org/10.1016/j.molliq.2020.113794.
[54] B. Chen, M. He, X. Zhang, W. Fei, Y. Cui, X. Guo, A novel method for fabrication of coated microneedles with homogeneous and controllable drug dosage for transdermal drug delivery, Drug Deliv. and Transl. Res. 12 (2022) 2730–2739, https://doi.org/10.1007/s13346-022-01123-8.
[55] Z. Chen, J. He, J. Qi, Q. Zhu, W. Wu, Y. Lu, Long-acting microneedles: a progress report of the state-of-the-art techniques, Drug Discov. Today 25 (2020) 1462–1468, https://doi.org/10.1016/j.drudis.2020.05.006.
[56] M. Kim, S. Park, S. Choi, Dual-nozzle spray deposition process for improving the stability of proteins in polymer microneedles, RSC Adv. 7 (2017) 55350–55359, https://doi.org/10.1039/C7RA10928H.
[57] R. Li, L. Zhang, X. Jiang, L. Li, S. Wu, X. Yuan, H. Cheng, X. Jiang, M. Gou, 3D-printed microneedle arrays for drug delivery, J. Contr. Release 350 (2022) 933–948, https://doi.org/10.1016/j.jconrel.2022.08.022.
[58] S. Xu, S. Ahmed, M. Momin, A. Hossain, T. Zhou, Unleashing the potential of 3D printing soft materials, Device 1 (2023) 100067, https://doi.org/10.1016/j.device.2023.100067.
[59] Z. Huang, X. Sun, P. Wang, H. Wan, Emerging single-atom catalysts in electrochemical biosensing, VIEW 4 (2023) 20220058, https://doi.org/10.1002/VIW.20220058.
[60] Y. Cheng, X. Gong, J. Yang, G. Zheng, Y. Zheng, Y. Li, Y. Xu, G. Nie, X. Xie, M. Chen, C. Yi, L. Jiang, A touch-actuated glucose sensor fully integrated with microneedle array and reverse iontophoresis for diabetes monitoring, Biosens. Bioelectron. 203 (2022) 114026, https://doi.org/10.1016/j.bios.2022.114026.
[61] X. Wang, W. Qiu, C. Lu, Z. Jiang, C. Hou, Y. Li, Y. Wang, H. Du, J. Zhou, X. Liu, Fabrication of flexible and conductive microneedle array electrodes from silk fibroin by mesoscopic engineering, Adv. Funct. Mater. 34 (2024) 2311535, https://doi.org/10.1002/adfm.202311535.
[62] L. Kong, H. Wen, Y. Luo, X. Chen, X. Sheng, Y. Liu, P. Chen, Dual-conductive and stiffness-morphing microneedle patch enables continuous in planta monitoring of electrophysiological signal and ion fluctuation, ACS Appl. Mater. Inter. 15 (2023) 43515–43523, https://doi.org/10.1021/acsami.3c08783.
[63] L. Sun, X. Zhu, X. Zhang, G. Chen, F. Bian, J. Wang, Q. Zhou, D. Wang, Y. Zhao, Induced cardiomyocytes-integrated conductive microneedle patch for treating myocardial infarction, Chem. Eng. J. 414 (2021) 128723, https://doi.org/10.1016/j.cej.2021.128723.
[64] S.M.A. Mokhtar, M. Yamada, T.W. Prow, M. Moore, X.L. Strudwick, D.R. Evans, PEDOT coated microneedles towards electrochemically assisted skin sampling, J. Mater. Chem. B 11 (2023) 5021–5031, https://doi.org/10.1039/d3tb00485f.
[65] B. Yang, X.E. Fang, J.L. Kong, Engineered microneedles for interstitial fluid cell-free DNA capture and sensing using iontophoretic dual-extraction wearable patch, Adv. Funct. Mater. 30 (2020) 2000591, https://doi.org/10.1002/adfm.202000591.
[66] S. Kusama, K. Sato, Y. Matsui, N. Kimura, H. Abe, S. Yoshida, M. Nishizawa, Transdermal electroosmotic flow generated by a porous microneedle array patch, Nat. Commun. 12 (2021) 658, https://doi.org/10.1038/s41467-021-20948-4.
[67] S. Yao, C. Zhang, J. Ping, Y. Ying, Recent advances in hydrogel microneedle-based biofluid extraction and detection in food and agriculture, Biosens. Bioelectron. 250 (2024) 116066, https://doi.org/10.1016/j.bios.2024.116066.
[68] Y. Wang, R. Thakur, Q. Fan, B. Michniak, Transdermal iontophoresis: combination strategies to improve transdermal iontophoretic drug delivery, Eur. J. Pharm. Biopharm. 60 (2005) 179–191, https://doi.org/10.1016/j.ejpb.2004.12.008.
[69] Y. Zheng, R. Ye, X. Gong, J. Yang, B. Liu, Y. Xu, G. Nie, X. Xie, L. Jiang, Iontophoresis-driven microneedle patch for the active transdermal delivery of vaccine macromolecules, Microsyst. Nanoeng. 9 (2023) 35, https://doi.org/10.1038/s41378-023-00515-1.
[70] D. Vora, H.T. Garimella, C.L. German, A.K. Banga, Microneedle and iontophoresis mediated delivery of methotrexate into and across healthy and psoriatic skin, Int. J. Pharmaceut. 618 (2022) 121693, https://doi.org/10.1016/j.ijpharm.2022.121693.
[71] M.S.A. Junaid, A.K. Banga, Transdermal delivery of baclofen using iontophoresis and microneedles, AAPS PharmSciTech 23 (2022) 84, https://doi.org/10.1208/s12249-022-02232-w.
[72] S. Xiao, Y. Yan, J. Zhao, Y. Zhang, N. Feng, Increased microneedle-mediated transdermal delivery of tetramethylpyrazine to the brain, combined with borneol and iontophoresis, for MCAO prevention, Int. J. Pharmaceut. 575 (2020) 118962, https://doi.org/10.1016/j.ijpharm.2019.118962.
[73] U. Detamornrat, M. Parrilla, J. Domínguez-Robles, Q.K. Anjani, E. Larrañeta, K. D. Wael, R.F. Donnelly, Transdermal on-demand drug delivery based on an iontophoretic hollow microneedle array system, Lab Chip 23 (2023) 2304–2315, https://doi.org/10.1039/d3lc00160a.
[74] M.S. Arshad, S. Hussain, S. Zafar, S.J. Rana, N. Ahmad, N.A. Jalil, Z. Ahmad, Improved transdermal delivery of rabies vaccine using iontophoresis coupled microneedle approach, Pharm. Res. 40 (2023) 2039–2049, https://doi.org/10.1007/s11095-023-03521-0.
[75] R.F. Donnelly, T.R.R. Singh, M.J. Garland, K. Migalska, R. Majithiya, C. M. McCrudden, P.L. Kole, T.M.T. Mahmood, H.O. McCarthy, A.D. Woolfson, Hydrogel-forming microneedle arrays for enhanced transdermal drug delivery, Adv. Funct. Mater. 22 (2012) 4879–4890, https://doi.org/10.1002/adfm.201200864.
[76] M. Peng, Z. Heng, D. Ma, B. Hou, K. Yang, Q. Liu, Z. Gu, W. Liu, S. Chen, Iontophoresis-integrated smart microneedle delivery platform for efficient transdermal delivery and on-demand insulin release, ACS Appl. Mater. Inter. 16 (2024) 70378–70391, https://doi.org/10.1021/acsami.4c18381.
[77] L. Zhang, R. Guo, S. Wang, X. Yang, G. Ling, P. Zhang, Fabrication, evaluation and applications of dissolving microneedles, Int. J. Pharmaceut. 604 (2021) 120749, https://doi.org/10.1016/j.ijpharm.2021.120749.
[78] K. Ita, Dissolving microneedles for transdermal drug delivery: advances and challenges, Biomed. Pharmacother. 93 (2017) 1116–1127, https://doi.org/10.1016/j.biopha.2017.07.019.
[79] J. Lee, J. Park, M. Prausnitz, Dissolving microneedles for transdermal drug delivery, Biomaterials 29 (2008) 2113–2124, https://doi.org/10.1016/j.biomaterials.2007.12.048.
[80] T. Bauleth-Ramos, N. El-Sayed, F. Fontana, M. Lobita, M.A. Shahbazi, H. A. Santos, Recent approaches for enhancing the performance of dissolving microneedles in drug delivery applications, Mater, Today Off. 63 (2023) 239–287, https://doi.org/10.1016/j.mattod.2022.12.007.
[81] Z. Sartawi, C. Blackshields, W. Faisal, Dissolving microneedles: applications and growing therapeutic potential, J. Contr. Release 348 (2022) 186–205, https://doi.org/10.1016/j.jconrel.2022.05.045.
[82] M. Abbasi, Z.Y. Fan, J.A. Dawson, S. Wang, Transdermal Delivery of Metformin Using Dissolving microneedles and iontophoresis patches for browning

subcutaneous adipose tissue, Pharmaceutics 14 (2022) 879, https://doi.org/10.3390/pharmaceutics14040879.
[83] M. Bok, Z.J. Zhao, S. Jeon, J.H. Jeong, E. Lim, Ultrasonically and iontophoretically enhanced drug-delivery system based on dissolving microneedle patches, Sci. Rep. 10 (2020) 2027, https://doi.org/10.1038/s41598-020-58822-w.
[84] K. Saepang, S.K. Li, D. Chantasart, Passive and iontophoretic transport of pramipexole dihydrochloride across human skin microchannels created by microneedles, Int. J. Pharmaceut. 609 (2021) 121092, https://doi.org/10.1016/j.ijpharm.2021.121092.
[85] D. Kang, Q. Ge, M.A. Natabou, W. Xu, X. Liu, B. Xu, X. Bao, Y.N. Kalia, Y. Chen, Bolus delivery of palonosetron through skin by tip-loaded dissolving microneedles with short-duration iontophoresis: a potential strategy to rapidly relieve emesis associated with chemotherapy, Int. J. Pharmaceut. 628 (2022) 122294, https://doi.org/10.1016/j.ijpharm.2022.122294.
[86] J.P. Ronnander, L. Simon, A. Koch, Transdermal delivery of sumatriptan succinate using iontophoresis and dissolving microneedles, J. Pharm. Sci. 108 (2019) 3649–3656, https://doi.org/10.1016/j.xphs.2019.07.020.
[87] G. Gao, L. Zhang, Z. Li, S. Ma, F. Ma, Porous microneedles for therapy and diagnosis: fabrication and challenges, ACS Biomater. Sci. Eng. 9 (2023) 85–105, https://doi.org/10.1021/acsbiomaterials.2c01123.
[88] W. Xue, J. Na, L. Zhang, Y. Zu, F. Lin, Developing porous microneedles patch for the detection of wound infections, Adv. Mater. Technol. 9 (2024) 2301572, https://doi.org/10.1002/admt.202301572.
[89] Y. Li, J. Yang, Y. Zheng, R. Ye, B. Liu, Y. Huang, W. Zhou, L. Jiang, Iontophoresis-driven porous microneedle array patch for active transdermal drug delivery, Acta Biomater. 121 (2021) 349–358, https://doi.org/10.1016/j.actbio.2020.12.023.
[90] M. Wang, G. Yan, Q. Xiao, N. Zhou, H. Chen, W. Xia, L. Peng, Iontophoresis-driven microneedle arrays delivering transgenic outer membrane vesicles in program that stimulates transcutaneous vaccination for cancer immunotherapy, Small Sci 3 (2023) 2300126, https://doi.org/10.1002/smsc.202300126.
[91] K. Nagamine, J. Kubota, H. Kai, Y. Ono, M. Nishizawa, An array of porous microneedles for transdermal monitoring of intercellular swelling, Biomed. Microdevices 19 (2017) 68, https://doi.org/10.1007/s10544-017-0207-y.
[92] H. Terui, N. Kimura, R. Segawa, S. Kusama, H. Abe, D. Terutsuki, K. Yamasaki, M. Nishizawa, Intradermal vaccination via electroosmotic injection from a porous microneedle patch, J. Drug Deliv. Sci. Tec. 75 (2022) 103711, https://doi.org/10.1016/j.jddst.2022.103711.
[93] H. Abe, K. Sato, N. Kimura, S. Kusama, D. Inoue, K. Yamasaki, M. Nishizawa, Porous microneedle patch for electroosmosis-promoted transdermal delivery of drugs and vaccines, Adv. Nanobiomed. Res. 2 (2022) 2100066, https://doi.org/10.1002/anbr.202100066.
[94] Y. Abe, N. Kimura, H. Konno, S. Yoshida, M. Nishizawa, Porous microneedle-based wearable device for monitoring of transepidermal potential, Biomed. Eng. Adv. 1 (2021) 100004, https://doi.org/10.1016/j.bea.2021.100004.
[95] G. Wang, K. Kato, S. Ichinose, D. Inoue, A. Kobayashi, H. Terui, S. Tottori, M. Kanzaki, M. Nishizawa, Bilaterally aligned electroosmotic flow generated by porous microneedle device for dual-mode delivery, Adv. Healthc. Mater. 13 (2024) 2401181, https://doi.org/10.1002/adhm.202401181.
[96] D. Terutsuki, R. Segawa, S. Kusama, H. Abe, M. Nishizawa, Frustoconical porous microneedle for electroosmotic transdermal drug delivery, J. Contr. Release 354 (2023) 694–700, https://doi.org/10.1016/j.jconrel.2023.01.055.
[97] G. Wang, K. Kato, I. Aoki, S. Ichinose, D. Inoue, S. Tottori, M. Nishizawa, Transdermal drug delivery using a porous microneedle device driven by a hydrogel electroosmotic pump, J. Mater. Chem. B 12 (2024) 1490–1494, https://doi.org/10.1039/d3tb02208k.
[98] O. Howells, N. Rajendran, S. Mcintyre, S. Amini-Asl, P. Henri, Y. Liu, O. Guy, A.E. G. Cass, M.C. Morris, S. Sharma, Microneedle array-based platforms for future theranostic applications, Chembiochem 20 (2019) 2198–2202, https://doi.org/10.1002/cbic.201900112.
[99] Y. Liu, L. Yang, Y. Cui, A wearable, rapidly manufacturable, stability-enhancing microneedle patch for closed-loop diabetes management, Microsyst. Nanoeng. 10 (2024) 112, https://doi.org/10.1038/s41378-024-00663-y.
[100] Y. Liu, Q. Yu, L. Ye, L. Yang, Y. Cui, A wearable, minimally-invasive, fully electrochemically-controlled feedback minisystem for diabetes management, Lab Chip 23 (2023) 421–436, https://doi.org/10.1039/d2lc00797e.
[101] C. Yang, T. Sheng, W. Hou, J. Zhang, L. Cheng, H. Wang, W. Liu, S. Wang, X. Yu, Y. Zhang, J. Yu, Z. Gu, Glucose-responsive microneedle patch for closed-loop dual-hormone delivery in mice and pigs, Sci. Adv. 8 (2022) eadd3197, https://doi.org/10.1126/sciadv.add3197.
[102] X. Luo, Q. Yu, Y. Liu, W. Gai, L. Ye, L. Yang, Y. Cui, Closed-loop diabetes minipatch based on a biosensor and an electroosmotic pump on hollow biodegradable microneedles, ACS Sens. 7 (2022) 1347–1360, https://doi.org/10.1021/acssensors.1c02337.
[103] X. Li, X. Huang, J. Mo, H. Wang, Q. Huang, C. Yang, T. Zhang, H. Chen, T. Hang, F. Liu, L. Jiang, Q. Wu, H. Li, N. Hu, X. Xie, A fully integrated closed-loop system based on mesoporous microneedles-iontophoresis for diabetes treatment, Adv. Sci. 8 (2021) 2100827, https://doi.org/10.1002/advs.202100827.
[104] J. Yang, S. Zheng, D. Ma, T. Zhang, X. Huang, S. Huang, H. Chen, J. Wang, L. Jiang, X. Xie, Masticatory system-inspired microneedle theranostic platform for intelligent and precise diabetic management, Sci. Adv. 8 (2022) eabo6900, https://doi.org/10.1126/sciadv.abo6900.
[105] M. Parrilla, U. Detamornrat, J. Dominguez-Robles, S. Tunca, R.F. Donnelly, K. De Wael, Wearable microneedle-based array patches for continuous electrochemical monitoring and drug delivery: toward a closed-loop system for methotrexate treatment, ACS Sens. 8 (2023) 4161–4170, https://doi.org/10.1021/acssensors.3c01381.
[106] H. Zhao, G. Liang, J. Xiong, X. Wang, X. Hu, Z. Wei, A closed-loop smart dressing based on microneedle and electrochemical micropump for early diagnosis and in-time therapy of chronic wound, Sens. Actuat. B: Chem. 417 (2024) 136092, https://doi.org/10.1016/j.snb.2024.136092.